AD-A123 740 SIGNAL COHERENCE MODELING FOR SHALLOW WATER WITH ROUGH BOUNDARIES(U) DEFENCE RESEARCH ESTABLISHMENT PACIFIC VICTORIA (BRITISH COLUMBIA) J M OZARD ET AL. MAR 82 1/1

UNCLASSIFIED DREP-TM-82-1 F/G 12/1 NL

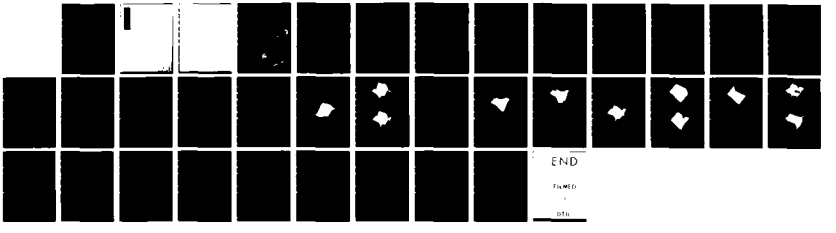

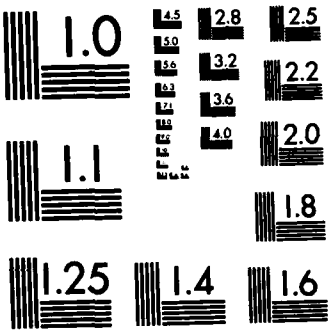

(6)

DEFENCE RESEARCH ESTABLISHMENT PACIFIC

VICTORIA, B.C.

Technical Memorandum 82-1

SIGNAL COHERENCE MODELING FOR SHALLOW WATER WITH ROUGH BOUNDARIES

by

J.M. Ozard, G.H. Brooke and M.J. Wilmut

January 1982

Approved by:

H. L. [illegible]

C/DREP

RESEARCH AND DEVELOPMENT BRANCH
DEPARTMENT OF NATIONAL DEFENCE
CANADA

Table of Contents

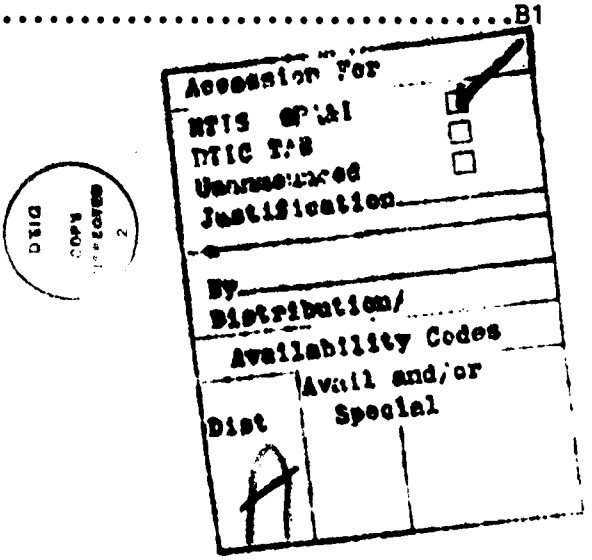

Abstract

A normal mode model is used to predict signal coherence for a sound source moving horizontally in shallow water. In the model, modal amplitude or modal phase are assumed to fluctuate. The fluctuations are ascribed to the effect of the surface or bottom roughness on sound propagation. For frequencies at which only a few modes are important, namely water depths of the order of 1.5 wavelengths, model coherence was calculated for sensor configurations in the plane containing source and receivers.

For source motion towards the receivers, it was found that for phase and amplitude fluctuations the coherences obtained are identical and that the coherence, which can drop to zero over a few wavelengths, is independent of the fluctuation distribution width. Thus it turns out that, for source motion towards the receivers, coherence is controlled by mode strengths and mode propagation constants. In contrast, if the source is in motion in a circle about a vertical array, coherence depends upon the distribution width, and for the same distribution width coherences for phase fluctuations are proportionately lower than those for amplitude fluctuations.

INTRODUCTION

Our long-term aim is to predict spatial signal coherence for an acoustic continuous wave source in shallow water. We are interested in situations where the shallow water surfaces - bottom, top, or both are rough enough to affect the sound propagation significantly. It is assumed that the surface roughness produces fluctuations of the mode amplitude or the mode phase. The effect of such fluctuations on signal coherence is our primary concern here. In particular we wish to model the signal coherence for those low frequencies at which only a few modes exist. Normal mode theory predicts[1] that sound will be propagated predominantly as trapped modes and that for sufficiently low frequencies only a few modes can exist. That the sound does indeed propagate as a few modes has been confirmed for at least one Arctic shallow water location[2,3].

Spatial coherence has been modeled by P.W. Smith, Jr. for deep ocean environments where a multipath model is appropriate[4]. This multipath model and others based on a multipath analysis such as that of Jobst[5] are computationally cumbersome for the low frequencies we are modeling. Recently U.E. Rupe described a model[6] for calculating phase coherence in a shallow water waveguide where the single frequency source had significant extent and the infinitesimal elements of the source were assumed to radiate incoherently. His model uses a mode analysis for the sound propagation, and in this respect it is similar to the model presented here. However his source is stationary and he only presents results for vertically separated receivers. The purpose of his model was to throw light on the relationship between source characteristics and received signal. Furthermore, roughness was limited to a small sinusoidal ripple on the surface.

In a regime with only a few modes present, a deterministic or statistical approach working directly from surface profiles could be attempted. Instead, to make the problem more tractable and to give the results more general significance, we assume that the roughness has produced fluctuations of mode amplitude or of mode phase but not both. The distribution of mode

amplitude or phase is our starting point. We assume a family of such distributions and draw conclusions that are general to the extent that the distributions are appropriate. The model does not relate the coherence to the roughness of the waveguide boundaries.

Our model enables a calculation of coherence for a sensor pair of arbitrary separation and for arbitrary excitation of the normal modes. However, in this report, only vertical and endfire-horizontal hydrophone pairs are considered, and source motion is restricted to being towards the array or perpendicular to the vertical plane containing the sound source and array. The coherence information calculated from the model enables a more informed definition of experiments to measure coherence under rough surface conditions. The model also indicates at what depths arrays might best be deployed to maximize gain or to investigate coherence. Furthermore the results also have some bearing on the choice of vertical, horizontal or inclined arrays and indicates what spacings might be most suitable in such arrays.

THEORY

The situation modeled is that of a single frequency sinusoidal sound source in shallow water. As shown in Figure 1, sound from the source is received by hydrophones that may be at any depth but must lie in the same vertical plane as the source. Source motion may be in the vertical plane containing the source and the receivers, or perpendicular to the plane, but motion is restricted to being horizontal. The sound propagation is modeled as trapped normal modes with fluctuations of phase or amplitude. These fluctuations are attributed to the rough overlying ice surface or the rough bottom.

The amplitude for the modes was calculated for a solid ice layer overlying water with a solid bottom. The sound velocities are shown in Figure 1. For the low frequency results presented, only two trapped slowly moving modes are present. In the modal analysis, energy travelling at higher speeds is associated with the bottom and, for such means of transmission, little energy is found in the water column. It has also been confirmed by experiment

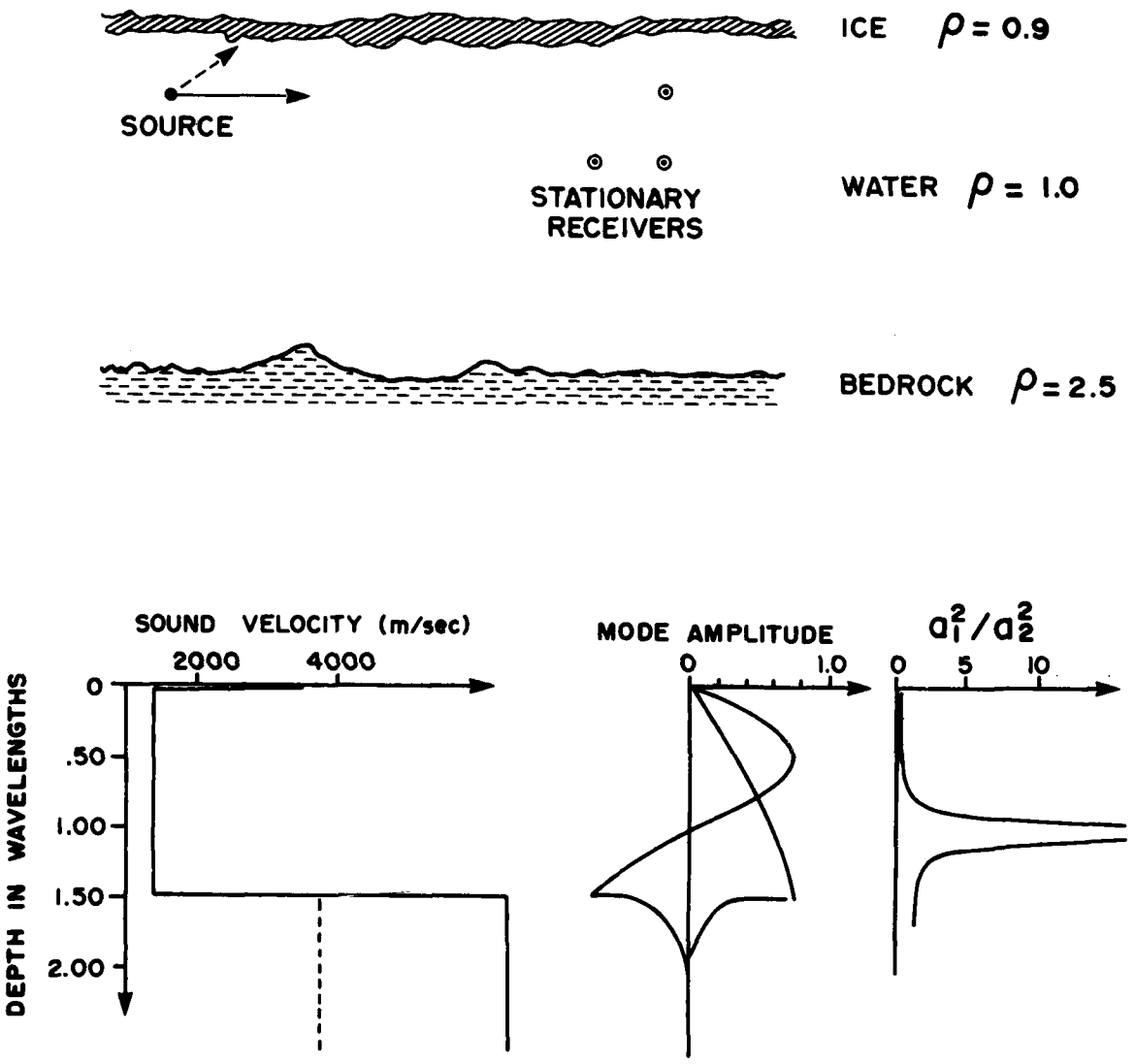

Figure 1. The geometry, physical parameters of the shallow water propagation model, and amplitudes of modes 1 and 2 are shown. Source motion is either in the plane containing source and receivers or perpendicular to the plane.

that the amount of energy propagated at these speeds is relatively insignificant compared to that propagated in the slowly moving modes[2]. For simplicity, the fast moving modes are ignored and only the slowly moving modes are included in the model.

Phases or amplitudes of the modes were considered to fluctuate as a result of the source moving through a waveguide of variable depth. The fluctuations were modeled by the distribution[7],

$$P(x) = \exp(K\cos x)/(2\ I_0(K)) \qquad -\infty < x < \infty$$

where $I_0(K)$ is the modified Bessel Function of the first kind order 0 and exp(x) denotes e^x. This distribution ranges from a uniform distribution for K=0, to the case where the phase is known when $K=\infty$. Figure 2 illustrates the shape of the distribution for several values of K. It can be seen that for K=10 the effective width of the distribution has already narrowed considerably from that for K=0.

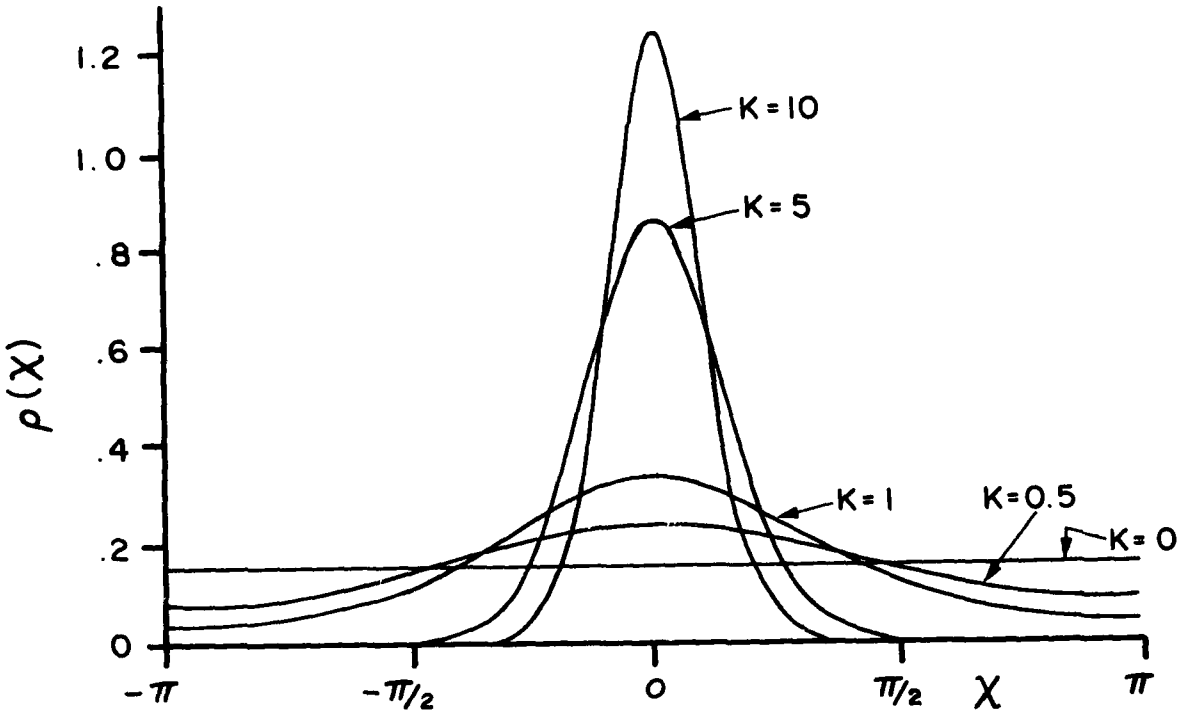

Figure 2. Shape of the fluctuation distribution for various values of K.

Coherence Assuming Phase Fluctuations

Numerous trapped normal modes and attenuating modes are generated at the source. In the model we consider only the slowly moving low frequency trapped modes that arrive at the receivers, and for each mode i we calculate from the normal mode model an amplitude and phase represented by the complex number a_i. This amplitude and phase is calculated at the source depth and the range of the first receiver. At the receiver depth an amplitude and phase represented by b_i for receiver 1 and c_i for receiver 2 is also calculated from the normal mode model. If we represent the Fourier transform of the input signal by $x_i(\omega)$ and assume no mode conversion in the vicinity of the receivers, we can write the output $Z_i(\omega)$ as,

$$Z_i(\omega) = \sum_{i=1}^{N} a_i b_i x_i(\omega) \tag{1}$$

where we have not as yet introduced fluctuations of phase produced by boundary roughness or other causes. The phase of each mode has a fluctuation which varies with the range of the source but is the same at each hydrophone. This implies that the receiver separation is small compared to the distance travelled by the source between successive realizations of the fluctuating phase. When the fluctuations are included, the received signal is

$$\begin{aligned} Z_1(\omega) &= \sum_{i=1}^{N} a_i b_i x_i(\omega)\exp(j\theta_i) \\ Z_2(\omega) &= \sum_{i=1}^{N} a_i c_i x_i(\omega)\exp(j\theta_i) \end{aligned} \tag{2}$$

where the distribution for θ_i is given by,

$$P(\theta_i) = \exp(K_i\cos\theta_i)/(2\pi I_o(K_i)). \tag{3}$$

In order to simplify the final result we replace the complex quantities a_i, b_i, c_i by their magnitude and phase. The phase shift for the a_i is that determined by the length of the propagation path from the sound source to the first receiver. This phase shift ϕ_i we associate with a_i as the phase shift affects the signal at both receivers. There is also a phase shift produced by the extra propagation path between receivers that is included in c_i.

Thus, a_i becomes $a_i\exp(i\phi_i)$

b_i becomes b_i

c_i becomes $c_i\exp(i\Theta)$

where a_i, b_i, c_i are real after the substitution. To calculate the coherence of the received signal we use the coherence definition,

$$\gamma^2(\omega) = \left|\overline{Z_1(\omega)\,Z_2^*(\omega)}\right|^2 / \left(\overline{|Z_1(\omega)|^2}\;\overline{|Z_2(\omega)|^2}\right) \tag{4}$$

where * denotes the complex conjugate and the bar denotes an ensemble average. For the case N=2, equations 2 and 3 were substituted into equation 4 and the integrations necessary to obtain expected values were carried out. For the case of horizontal source motion perpendicular to the line joining source and receivers, which will be called circumferential motion, the integrations are described in Appendix A. Thus,

$$\gamma^2(\omega) = \frac{\left|\begin{array}{l} a_1^2b_1c_1\exp(j\Theta_1)+\Delta_{12}[a_1b_1a_2c_2\exp j(\phi_2-\phi_1+\Theta_2) \\ +\,a_2b_2a_1c_1\exp j(\phi_1-\phi_2+\Theta_1)]+a_2^2b_2c_2\exp(j\Theta_2)\end{array}\right|^2}{\left|\begin{array}{l} a_1^2b_1^2+2\Delta_{12}a_1b_1a_2b_2\cos(\phi_1-\phi_2)+a_2^2b_2^2 \\ \left|\,a_1^2c_1^2+2\Delta_{12}a_1c_1a_2c_2\cos(\phi_1-\phi_2+\Theta_1-\Theta_2)+a_2^2c_2^2\,\right|\end{array}\right|}. \tag{5}$$

$$\Delta_{12} = \frac{I_1(K_1)I_1(K_2)}{I_o(K_1)I_o(K_2)}$$

In the event that source motion is horizontal and in the plane of the source and receivers, which we call radial source motion, then a further integration is required over the variable $\phi_1 - \phi_2$ in the evaluation of the expected values of the coherence. When the integration is carried out over an integral number of periods, terms in Equation 5 that contain Δ_{ij} will drop out for $i \neq j$. Consequently, for radial motion, signal coherence is not affected by phase fluctuations and therefore does not depend on how the fluctuations are distributed. The resulting coherence is that given by Equation 5 when K=0 since $\Delta_{j,i}=0$ if K=0.

The requirement that we integrate over an integral number of periods of $\phi_1 - \phi_2$ implies that in an experiment to obtain a coherence estimate, the measurement must be carried out over the period taken for an integral number or a very large number of mode interference maxima to pass from the first receiver to the second receiver.

Further simplification of Equation 5 for the case of radial motion shows that, in the expression for the phase shift, the receiver separation only occurs as the argument of a cosine function. Thus the coherence shows a cosinusoidal dependence on sensor separation. In fact, the model predicts that the coherence would periodically peak at unity as the receiver separation increases. However, in practice the assumptions of the model would not be satisfied and at large separations the coherence would peak at less than unity.

Coherence Assuming Amplitude Fluctuations

In the case of amplitude fluctuations the amplitude a_1 of the first mode was assumed to be distributed as,

$$P(a_1^2) = \frac{\exp[K\cos(\pi(a_1^2-\alpha)/\alpha)]}{2\alpha I_o(K)} \qquad (6)$$

where, $0 \leq a_1^2 \leq 2$.

It was also assumed that the sum of the energies in the two allowed modes at the source depth is constant,

$$a_2^2 = 1-a_1^2.$$

This was thought to be reasonable and was computationally convenient. Consequently, whereas for phase fluctuations a different distribution width can be used for each mode, for amplitude fluctuations the model only allows identical distributions for each mode. In a manner analogous to that for phase fluctuations, Equations 2 and 6 are substituted into Equation 4 and the integrations carried out as described in Appendix B. For the case of two modes and circumferential source motion the coherence is,

$$\gamma^2(\omega) = \frac{\left|\alpha b_1 c_1 \exp(j\theta_1)+b_1 c_2 \beta \exp j(\phi_2-\phi_1+\theta_2)\right.}{\left.+\, b_2 c_1 \beta \exp j(\phi_1-\phi_2+\theta_1)+(1-\alpha) b_2 c_2 \exp(j\theta_2)\right|^2} \qquad (7)$$

$$\frac{}{\left[\alpha b_1^2+2\beta b_1 b_2 \cos(\phi_1-\phi_2)+(1-\alpha) b_2^2\right] \cdot}$$

$$\left[\alpha c_1^2+2\beta c_1 c_2 \cos(\phi_1-\phi_2+\theta_1-\theta_2)+(1-\alpha) c_2^2\right]$$

where $\beta = \pi/8+\left[1/(2I_o(K))\right] \sum_{n=1}^{\infty} J_1(\pi n) I_n(K)/n$

As for phase fluctuations, simplification of Equation 7 reveals that the coherence is a cosinusoidal function of the receiver separation.

In the case of radial source motion, integration over an integral number of periods of the variable $\phi_1 - \phi_2$ is required. As a consequence of the cosinusoidal dependence on $\phi_1 - \phi_2$, all terms containing β have a zero coefficient in Equation 7. Therefore, as in the case of phase fluctuations, the coherence is independent of whether or not amplitude fluctuations are present or how fluctuations are distributed.

TECHNIQUES OF NUMERICAL EVALUATION

Because the calculations involved in Equation 5 and 7 require the difference of two nearly equal quantities, special care must be taken with significant digits. This is particularly true in the evaluation of the modified Bessel Function I(K) for large arguments and in the evaluation of β in Equation 7. Coefficients for calculating I(K) were taken from the Handbook of Mathematical Functions[8] and β was evaluated with Simpson's rule. The time required to calculate signal coherence is sufficiently small that a grid of 22,500 coherence values can be calculated and plotted in a few minutes. Consequently it was feasible to produce a catalogue of coherence plots to investigate how factors such as sensor separation, sensor depths, distribution widths, energy distribution between modes and source-receiver separation affect coherence. In this way coherence properties not immediately apparent from Equations 5 and 7 were investigated.

DISCUSSION OF RESULTS

Presentation of results is simplified by the similarities between coherences assuming phase fluctuations and those assuming amplitude fluctuations. For radial source motion the results are, in fact, identical regardless of the type of fluctuation and only one case needs to be presented.

When the source is in circumferential motion the coherence is the same for amplitude and phase fluctuations provided that $\frac{\beta}{a_1 a_2} = \Delta_{12}$ as can be seen from Equations 5 and 7. In this case only coherences for phase fluctuations need be presented. To evaluate the coherence for a given K and a_1^2 for the case of amplitude fluctuations the equivalent K value for phase fluctuations is found as illustrated in Figure 3.

The results presented below are those for phase fluctuations. Those for amplitude fluctuations are very similar and can be easily deduced. For example it can be seen from Figure 3 that coherences for amplitude fluctuations for K=0.1 and $a_1^2 = 0.3$ are equivalent to those for K=10 for phase fluctuations. Since coherence increases with increasing K, this means that coherences for amplitude fluctuations start at higher values and remain higher than those for phase fluctuations. This higher coherence for given K and the dependence of coherence upon the relative energy in the modes are the only differences between the coherences predicted for modes with fluctuating phase and those with fluctuating amplitude.

Coherence for Radial Source Motion

As mentioned earlier Equations 5 and 7 lose all dependence upon the distribution width for radial source motion. In fact, Equations 5 and 7 reduce to the same result, so that calculated coherences for amplitude or phase fluctuations are identical. These simplifications for radial source motion mean that coherence will depend only on source depth, receiver depths, signal frequency, and receiver separation. Put another way this implies that for radial source motion, the coherence depends only on receiver separation and the relative energy in the two modes at the receiver depths.

(a) Horizontal Separation of Receivers

Figure 4 illustrates the coherence (squared) as a function of separation for the situation in which the modes are equally excited. At a depth corresponding to a zero of one of the modes the coherence is unity, as shown in Figure 4 and, as the depth changes from the zero, the total energies in the two modes approach one another and the coherence deteriorates. At equality of the energies, which occurs at a depth of 0.80 or 1.50

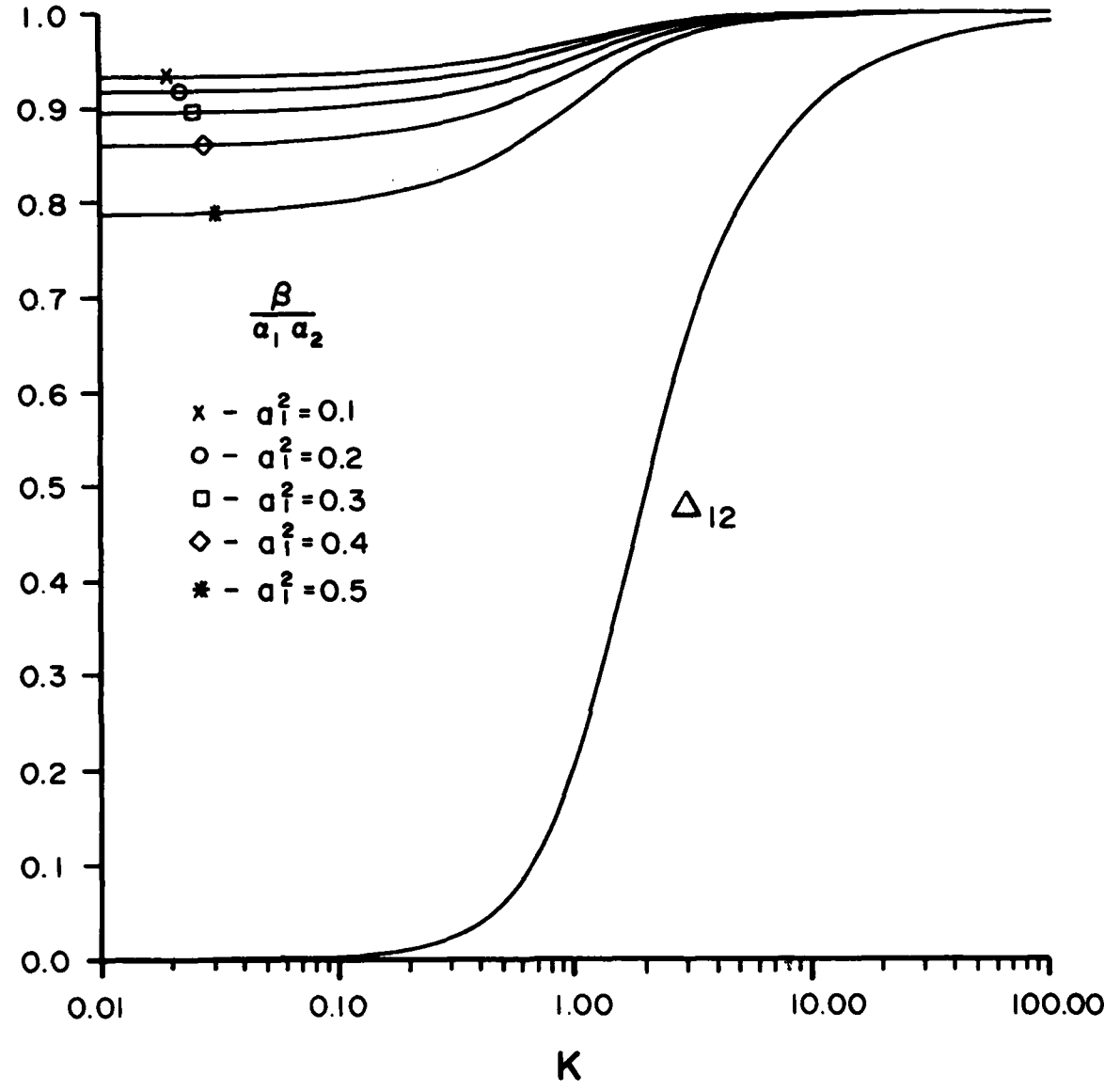

Figure 3. The graphs give the value of $\frac{\beta}{a_1 a_2}$ as a function of K and a_1^2 for amplitude fluctuations and Δ_{12} as a function of K for phase fluctuations. Equal values of $\frac{\beta}{a_1 a_2}$ and Δ_{12} produce identical coherences. Horizontal lines will intercept the $\frac{\beta}{a_1 a_2}$ and Δ_{12} curves for parameter values that produce equal coherences for circumferential motion.

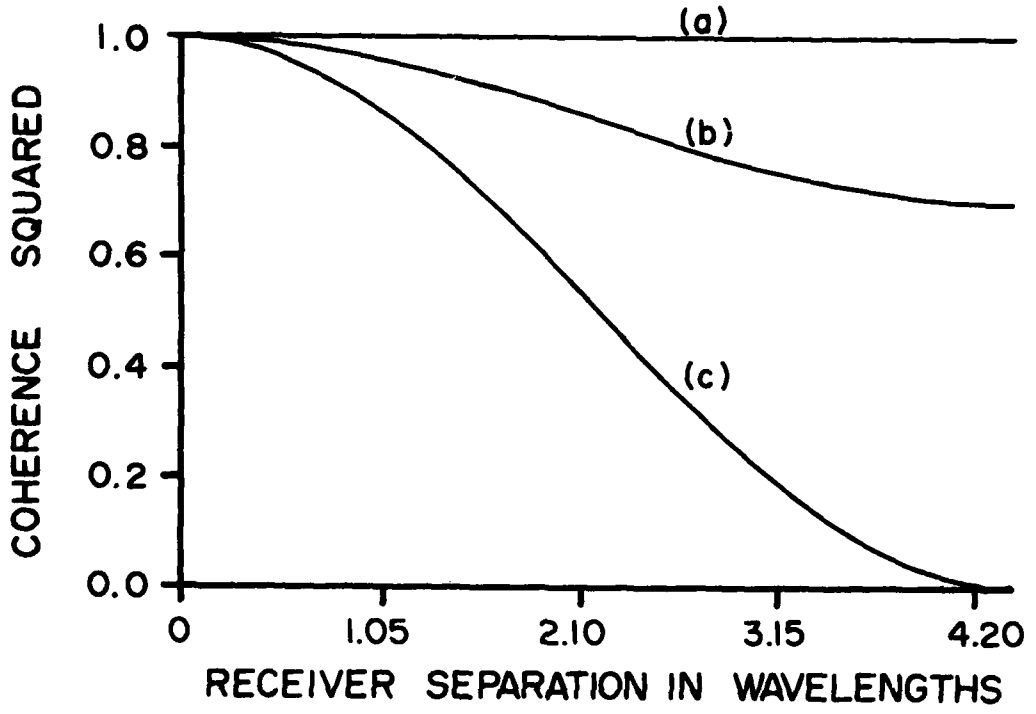

Figure 4. Coherence squared is plotted for a source moving towards two horizontally separated receivers (a) at a zero of the second mode, (b) near the surface and (c) at 0.80 or 1.50 wavelengths depth. The water depth is 1.5 wavelengths and $a_1^2 = 0.5$.

wavelengths, the coherence becomes zero when the receiver separation is 4.2 wavelengths or the phase shift $\theta_1-\theta_2$ is 360°. The theory predicts that the cosinusoidal curves shown in Figure 4 recover to unity over the next 4.2 wavelengths. However the assumptions on which the theory is based are violated at larger separations so that estimates of coherence would be too large for these larger separations.

A continuous plot of coherence against depth for horizontally separated receivers in water of 1.5 wavelengths depth is presented in Figures 5, 6 and 7. Coherences on the diagonal correspond to those for a horizontal separation of 4.2 wavelengths. At closer separations the coherences will be larger as illustrated by Figure 5. In the next two paragraphs these coherences on the diagonal, Z1=Z2, will be discussed.

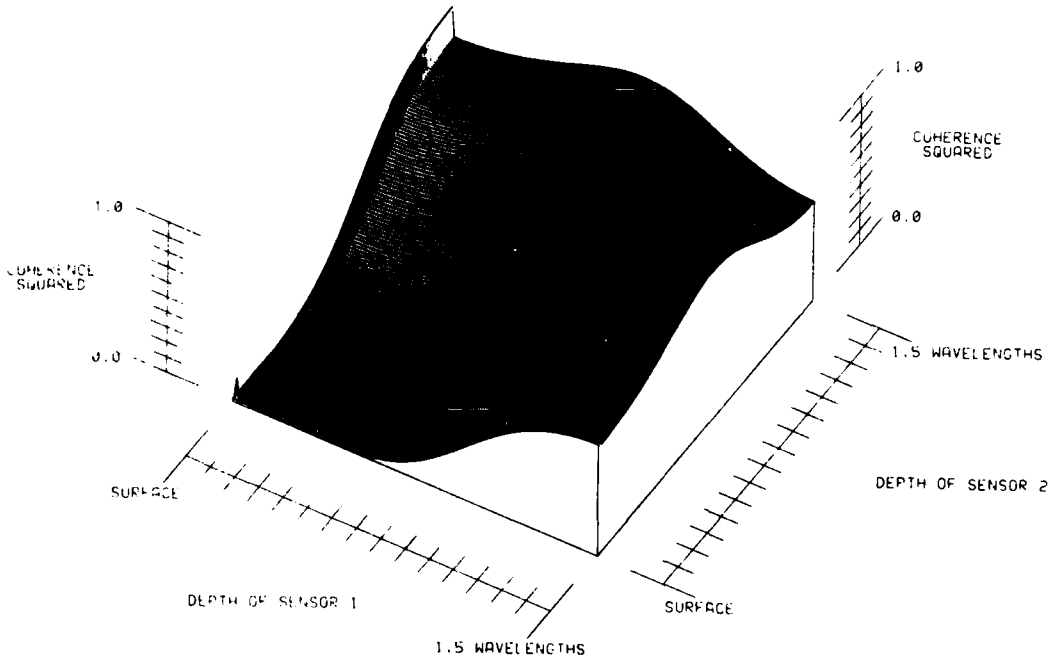

Figure 5. Coherence squared for a sound source at a depth of 1 wavelength (a_1^2/a_2^2 = 9, i.e near zero of second mode). The source is moving horizontally in the vertical plane containing source and receivers. A water depth of 1.5 wavelengths, a horizontal hydrophone separation of 4.2 wavelengths and phase fluctuations are assumed with K=0.

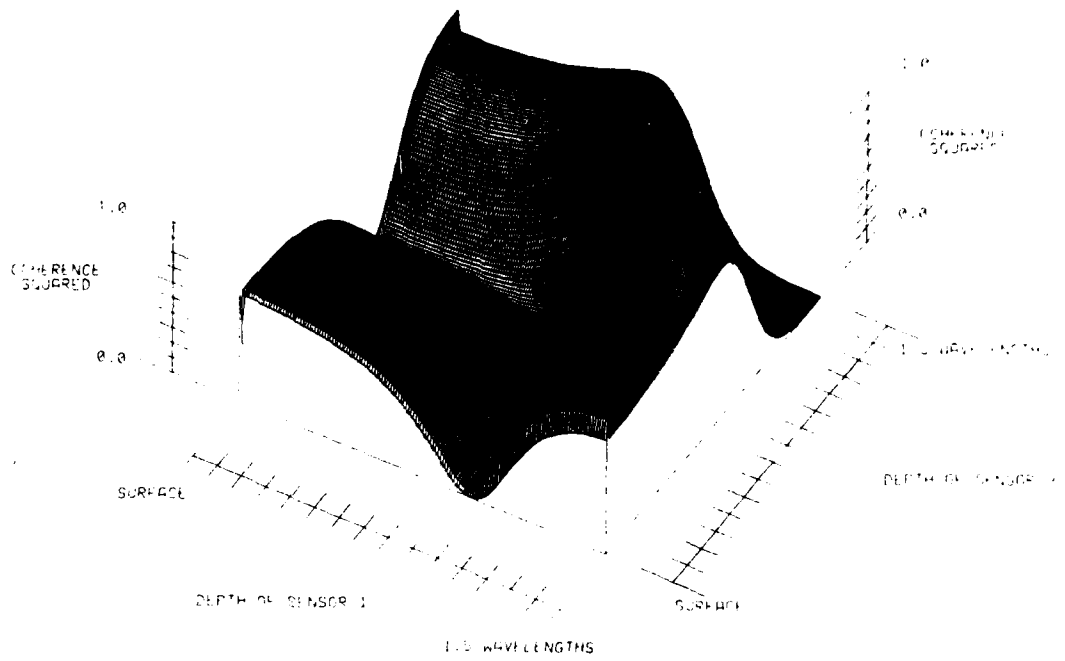

Figure 6. Coherence squared for a sound source at a depth of 1.2 to 1.5 wavelengths (a_1^2/a_2^2 = 1, i.e. near the bottom). The source is moving horizontally in the vertical plane containing source and receivers. A water depth of 1.5 wavelengths, a horizontal hydrophone separation of 4.2 wavelengths and phase fluctuations are assumed with K=0.

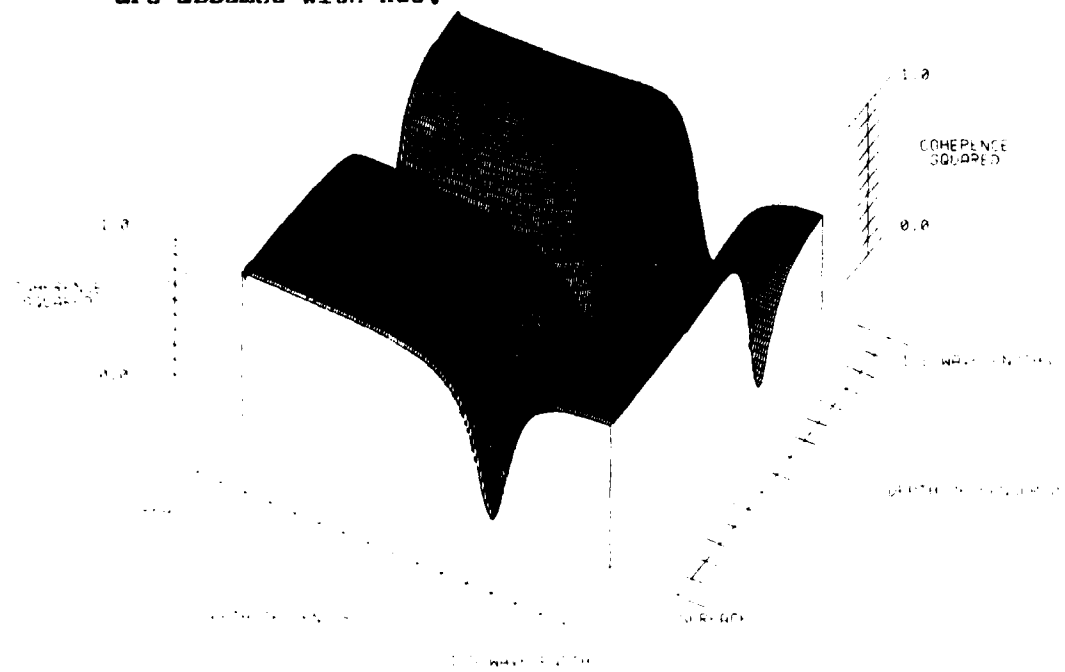

Figure 7. Coherence squared for a sound source in the upper half of the water column (a_2^2/a_1^2 = 9). The source is moving horizontally in the vertical plane containing source and receivers. A water depth of 1.5 wavelengths, a horizontal hydrophone separation of 4.2 wavelengths and phase fluctuations are assumed with K=0.

If the bottom is horizontal and the bottom roughness is sufficiently small compared to a wavelength mode conversion is unlikely. If there is no mode conversion, Figure 5 represents the modeled signal coherence for a source in the vicinity of the zero of the second mode at a depth of 1.04 wavelengths. The source depth can be determined from a_1^2/a_2^2 by consulting Figure 1. Similarly Figure 6 represents signal coherence for a source near the bottom while Figure 7 applies to a near surface source.

From the model results we see that for horizontally separated sensors near the zero of the second mode, the coherence is near unity while that for receivers near the bottom or top can be zero. Differences of depth from the zero of the mode of about 0.1 wavelengths would not significantly change the coherence from unity.

(b) Simulations Vertical and Horizontal Separation of Receivers

Examination of points off the diagonal in Figures 5, 6 and 7 reveals that there are pairs of depths almost symmetrically displaced above and below the zero of the second mode at 1 wavelength depth that always show good coherence. This occurs because the 180° phase shift brought about by the horizontal hydrophone separation is completely compensated by the phase reversal that results from the vertical separation of the two hydrophones above and below the zero of the second mode. The depths are not exactly symmetric about 1 wavelength because the first mode strength changes slowly with depth and the second mode is not exactly antisymmetric about the zero.

(c) Vertical Separation of Receivers

Figures 8, 9 and 10 show coherence for vertically separated sensors with no horizontal separation. Therefore, the useful information occurs off the diagonal $Z_1=Z_2$. Figures 8, 9 and 10 parallel the source depths of Figures 5, 6 and 7. For radial source motion it can be seen that good coherence can be obtained regardless of the source depth for sensors near the bottom or near the surface. Assuming no mode conversion, the range of depth pairs that give good coherence is usually larger at the surface, especially for a sound source just below the surface (Figure 8). Good coherence can be expected over an array up to 0.6 wavelengths long suspended just below the surface regardless of source depth.

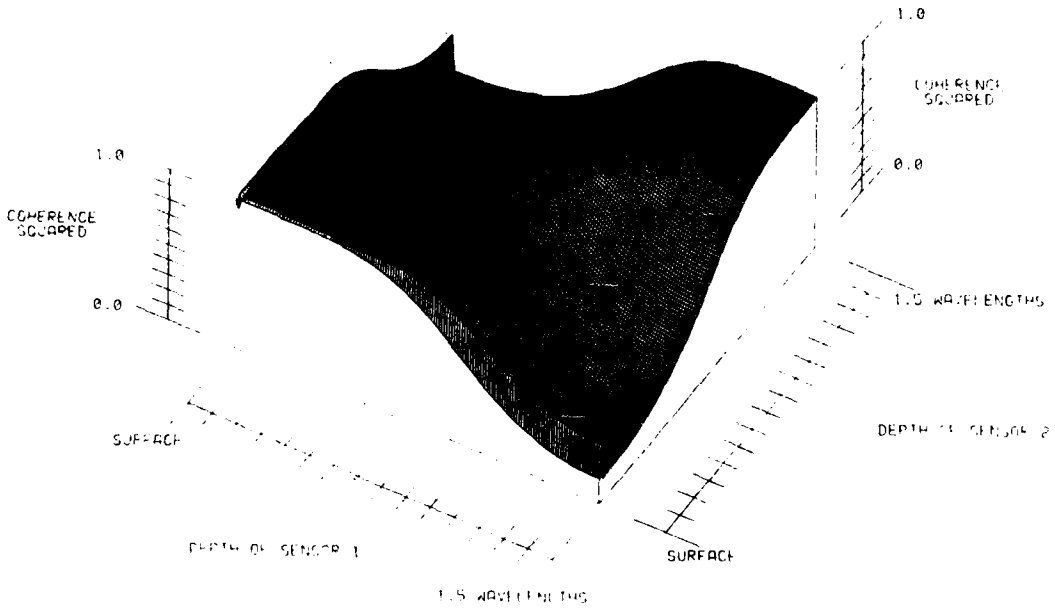

Figure 8. Coherence squared for a sound source moving horizontally in the vertical plane containing source and receivers. Motion is towards a pair of receivers that only have vertical separation. The source depth is approximately 1 wavelength ($a_1^2/a_2^2 = 9$, i.e. near the zero of the second mode). Phase fluctuations with K=0 and a water depth of 1.5 wavelengths are assumed.

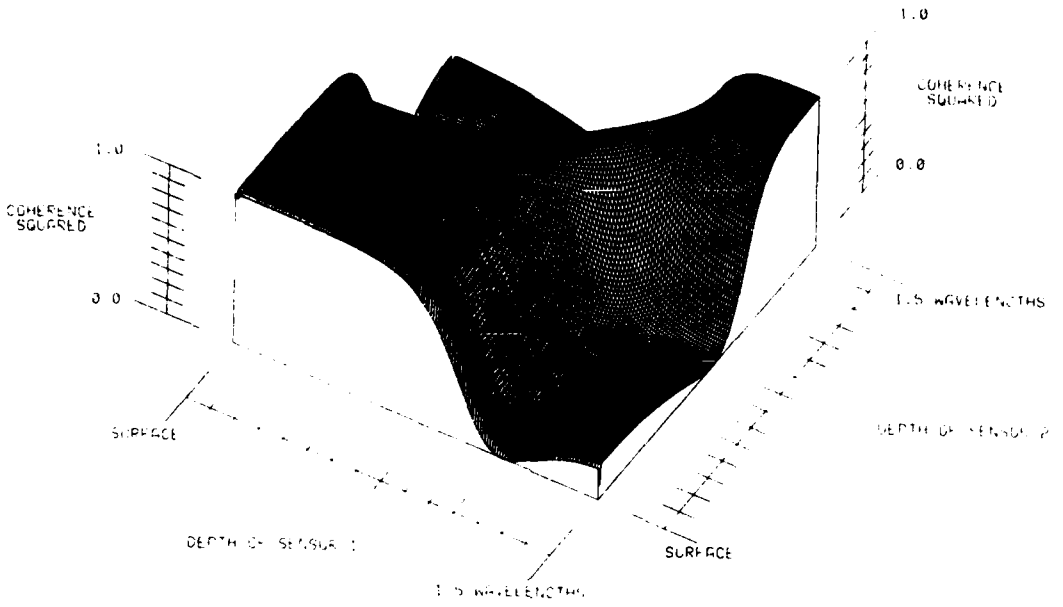

Figure 9. Coherence squared for a sound source moving horizontally in the vertical plane containing source and receivers. Motion is towards a pair of receivers that have only vertical separation. The source is near the bottom ($a_1^2/a_2^2 = 1$) in water 1.5 wavelengths deep. Phase fluctuations with K=0 are assumed.

Coherence for Circumferential Source Motion

For radial source motion coherence depends upon the receiver separation and relative energy in the two modes. However, for circumferential motion, coherence also depends upon the distribution width, type of fluctuation, and distance from the source to the first receiver. The relationship between coherences assuming phase fluctuations and that assuming amplitude fluctuations was discussed earlier so that only the phase fluctuation case need be discussed here. Coherence for vertically and for horizontally spaced receivers is discussed in the following paragraphs. With all of the possible arbitrary receiver configurations with vertical and horizontal separation only those of special interest are considered.

(a) Horizontal Separation of Receivers

Figures 11, 12 and 13 illustrate coherence for receivers on the bottom assuming circumferential source motion. Coherences for three source receiver ranges are shown. The parameter K, which determines the fluctuation distribution width as illustrated in Figure 2, is varied for each range. The curve for K=0 is cosinusoidal and represents the coherence that would be measured for circumferential motion at K=0, or for radial motion and any K. Clearly the coherence for circumferential motion, $K \geq 0$, departs significantly from that for radial motion. Space does not permit a reproduction of the coherences for all possible depths and ranges. However the results for other depths and ranges are indicated by the results in section (c) below.

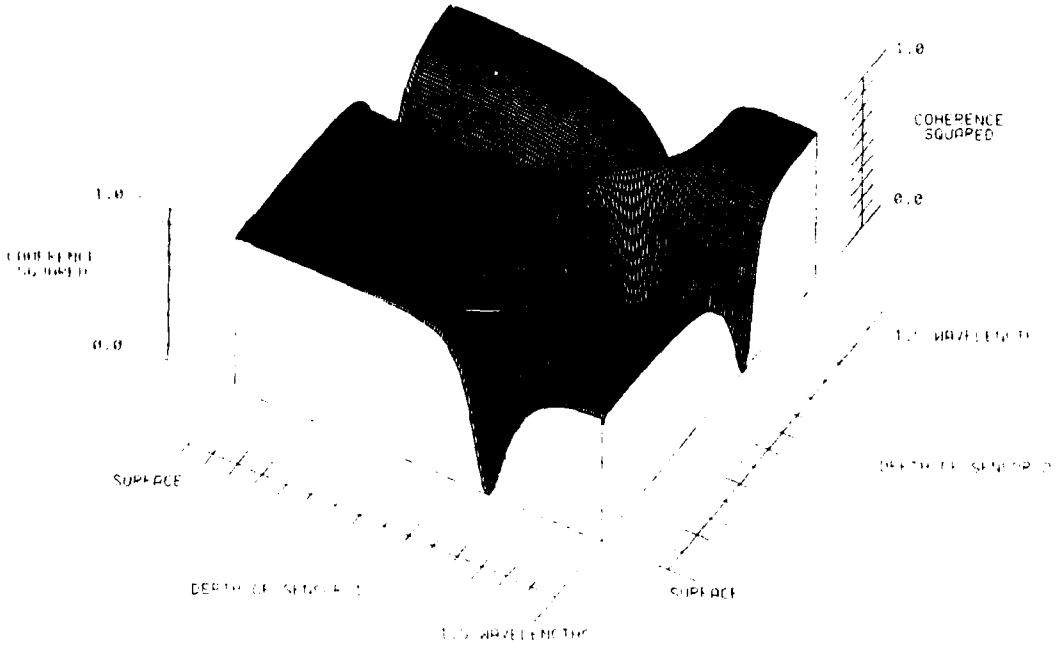

Figure 10. Coherence squared for a sound source moving horizontally in the vertical plane containing source and receivers. Motion is towards a pair of receivers that have only vertical separation. The source is in the upper half of the water column (a_2^2/a_1^2 = 9) in water 1.5 wavelengths deep and phase fluctuations with K=0 are assumed.

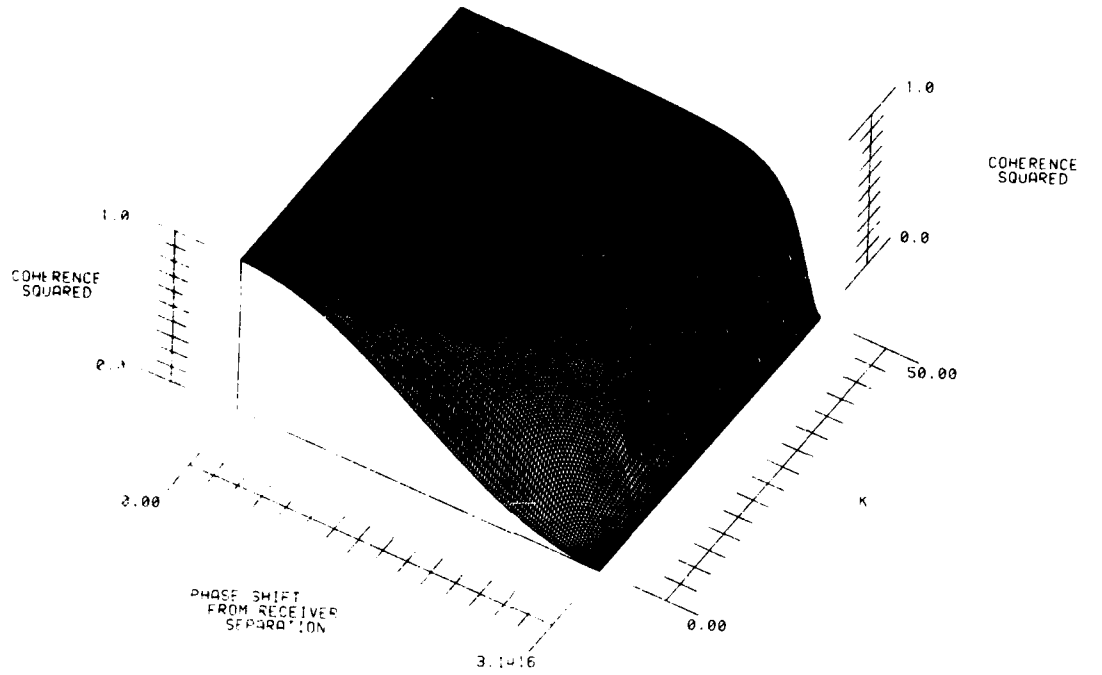

Figure 11. Coherence squared for a source near the bottom moving perpendicular to the vertical plane containing the source and receivers. The modes are in phase at the first receiver, $a_1^2/a_2^2 = 1$, and the receivers are on the bottom in water 1.5 wavelengths deep. Phase fluctuations are assumed.

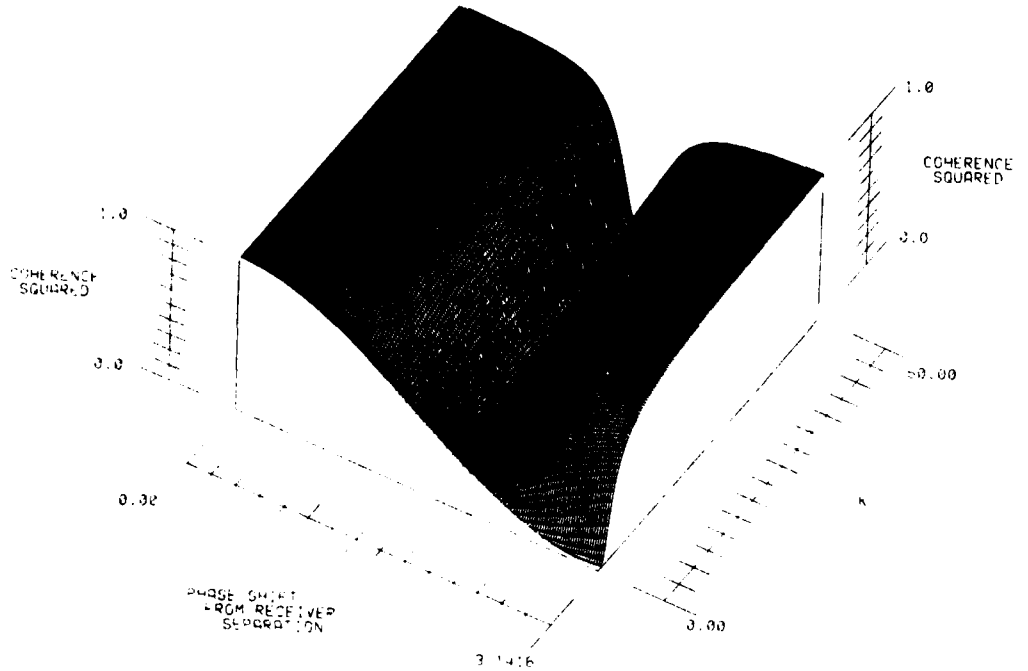

Figure 12. Coherence squared for a source near the bottom moving perpendicular to the vertical plane containing the source and receivers. The modes are a quarter wavelength out of phase at the first receiver, $a_1^2/a_2^2 = 1$, and the receivers are on the bottom. Water depth is 1.5 wavelengths deep and phase fluctuations are assumed.

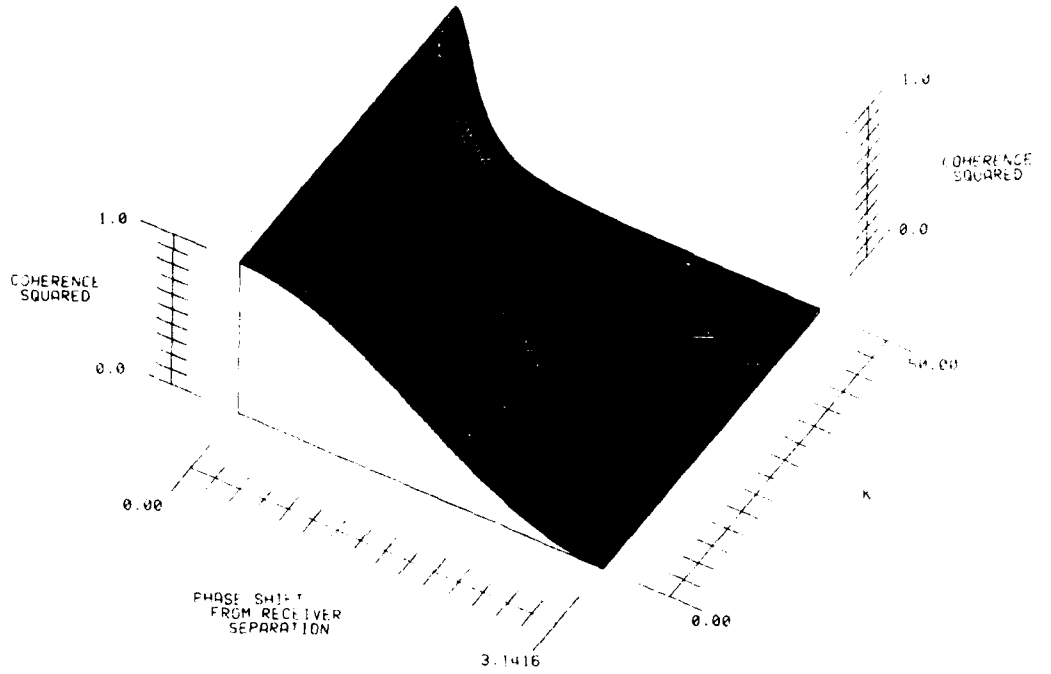

Figure 13. Coherence squared for a source near the bottom moving perpendicular to the vertical plane containing the source and receivers. The modes are a half wavelength out of phase at the first receiver, $a_1^2/a_2^2 = 1$, and the receivers are on the bottom. Water depth is 1.5 wavelengths and phase fluctuations are assumed.

(b) Vertical Separation of Receivers

From an examination of a large number of coherence plots three results can be stated regardless of relative mode strength at the receivers. Firstly, as the distribution narrows, i.e. as K increases, the mean coherence for all depth pairs increases. Secondly, as the range phase shift ($\phi_1-\phi_2$) between the modes increases to 360°, the range of depths extending down from the surface over which coherence is high increases. This is illustrated by Figures 14 and 15. Thirdly, as K increases, the coherence becomes more sensitive to the range phase shift between the modes.

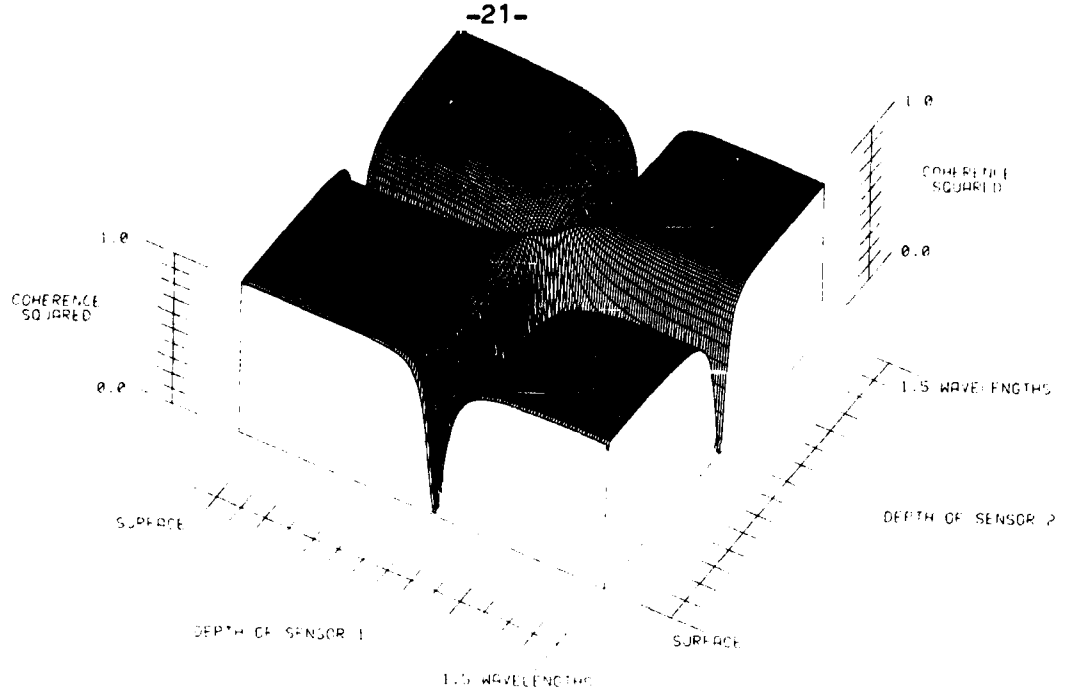

Figure 14. Coherence squared for vertically separated receivers and a source moving perpendicular to the vertical plane containing source and receivers. The modes are in phase at the first receiver and $a_1^2/a_2^2 = 1$ corresponding to a source near the bottom in water of 1.5 wavelengths depth. Phase fluctuations with K=50 are assumed.

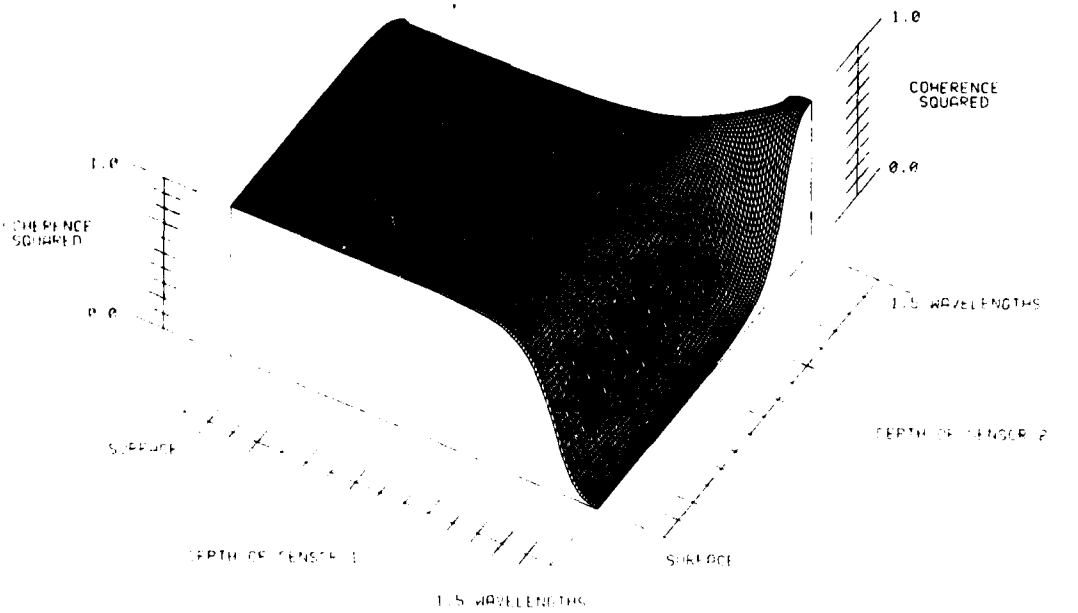

Figure 15. Coherence squared for vertically separated receivers and a source moving perpendicular to the vertical plane containing source and receivers. The modes are a half wavelength out of phase at the first receiver and $a_1^2/a_2^2 = 1$ corresponding to a source near the bottom in water 1.5 wavelengths deep. Phase fluctuations with K=50 are assumed.

Coherences for signals received by a vertical array with circumferential source motion can be used as a measure of the fluctuation distribution width. A narrow distribution is associated with good coherence over at least the upper 0.6 wavelengths. A strong dependence of coherence on the range between source and receivers is also indicative of a narrow distribution.

(c) Simultaneous Vertical and Horizontal Separation of Receivers

For circumferential source motion about an array of receivers with vertical and horizontal separation three results were found. As for a purely vertical array, mean coherence and sensitivity of the coherence to the phase shift between the modes increases with decreasing distribution width. On the other hand, the region of good coherence always found for a purely vertical array is not always present below the surface if the receivers have both vertical and horizontal separation.

MODEL IMPLICATIONS FOR SIGNAL COHERENCE MEASUREMENTS

Under conditions for which the model is appropriate, it indicates what sort of coherences we can expect over the octave bands for which the water depth is of the order of 1.5 wavelengths. At such frequencies the sound is propagated by a few modes with very different phase velocities and it is best modeled as modal propagation. In this report it has been shown that coherence depends upon numerous parameters and that in order to investigate signal coherence experimentally it is necessary to isolate conditions under which the value of these parameters can be determined.

The results of the study suggest that a vertical array with sensors approximately 0.2 wavelengths apart over the whole water column and a horizontal array four to eight wavelengths long should enable the parameters of the model to be measured. In order to resolve expected coherence variations the vertical array spacing should be less than 0.2 wavelengths near the zero of the second mode and larger elsewhere. Six hydrophones in each array should be sufficient. This array configuration should also be appropriate for measuring signal coherence in shallow water. Such arrays span those spacings over which signal coherence is likely to be high and therefore would also be suitable for providing some array gain.

In an experiment to investigate signal coherence radial source motions would enable the relative mode strengths and mode propagation constants to be measured while circumferential motion would enable the distribution width to be measured. For radial source motion experimental measurements can be carried out for any practical sensor configuration, and long straight tracks may be used. However for circumferential motion circular tracks centered on the receivers can be used only for vertical arrays. For horizontal arrays circumferential motion can be approximated by motion on circular paths of large radius centered on the receivers. The circular path must however be short so that the source remains near the end-fire position relative to the receivers. In this way sufficient samples can be collected to make a reasonably precise estimate of the coherence.

CONCLUSIONS

The model has enabled the calculation of an extensive set of signal coherences for endfire horizontal arrays and for vertical arrays. Without knowing the precise way in which phase or amplitude fluctuate certain general coherence results have been obtained. These are applicable to shallow water in the vicinity of 1.5 wavelengths depth. It has also been suggested that a vertical array through the water column and a horizontal array a few wavelengths long should enable the modal properties and fluctuation parameters to be defined.

Several general coherence results were obtained for the shallow water regime. Horizontal source motion in the vertical plane containing source and receivers produces coherence values which do not depend on the distribution width and are independent of whether phase or amplitude fluctuations are assumed. In contrast the generally higher coherences for source motion perpendicular to the plane containing source and receivers depends upon the type of fluctuation and the fluctuation distribution width. It was also found that the lowest coherences that can be obtained assuming phase fluctuations are substantially lower than can be obtained assuming amplitude fluctuations. For either type of motion coherence loss

for horizontally separated hydrophones occurs over a few wavelengths. For vertical arrays good coherence regions are found near the surface and in the vicinity of the zeros of the modes.

The model is not likely to be valid for hydrophone separations greater than a few wavelengths nor at substantially higher frequencies, for which a greater number of propagating modes exist. However for pairs of higher order modes, still at low frequencies, the coherence will show similar characteristics repeated through the water column a number of times equal to the number of zeros in the higher order modes.

REFERENCES

1. C.L. Pekeris, "Theory of Propagation of Explosive Sound in Shallow Water", in "Propagation of Sound in the Ocean", Geol. Soc. of Am., Memoir 27, 1948.

2. R.F. MacKinnon, G.H. Brooke and J.M. Ozard, "Propagation Anomalies in Shallow Arctic Water", (Abstract), J. Acoust. Soc. Am., 69, Sup 1, H7, 1981.

3. R.F. MacKinnon and J.M. Ozard, "Low-Frequency Shallow Water Propagation in Barrow Strait, N.W.T., Canada", (Abstract), J. Acoust. Soc. Am., 60 Sup 1, P 17, 1976.

4. P.W. Smith, Jr., "Spatial Coherence in Multipath or Multimodal Channels", J. Acoust. Soc. Am., 60, 305-310, 1976.

5. J. Jobst, "An Application of Poisson Process Models to Multipath Sound Propagation of Sinusoidal Signals", J. Acoust. Soc. Am., 57, pp 1409-1412, 1975.

6. E. Rupe, "Phase Coherence in a Shallow Water Waveguide", in "Bottom-Interacting Ocean Acoustics", Ed. W.A. Kuperman and F.B. Jensen, NATO Conference Series IV, Marine Sciences, 1980.

7. H.L. VanTrees, "Detection Estimation and Modulation Theory", Part 1, 338, John Wiley and Sons Inc., N.Y., 1968.

8. M. Abramowitz and I.A. Stegun, "Handbook of Mathematical Functions", Dover Publications Inc., N.Y., 1965.

9. I.S. Gradshteyn and I.M. Ryzhik, "Table of Integrals, Series and Products", Academic Press, N.Y., 1965.

APPENDIX A

COHERENCE SQUARED FOR PHASE FLUCTUATIONS

From equation 2

$$Z_1 Z_1^* = \sum_{i,k,l,m=1}^{N} b_i a_k b_l^* a_m^* \delta_{ik} \delta_{ml} e^{j\theta k} e^{-j\theta m} \tag{A1}$$

where θ is the fluctuating phase distributed as defined by $P(\theta)$ Equation 3, and $\delta_{ik}\delta_{ml}$ implies no mode conversion in the vicinity of the receivers, simplifying A1 we have

$$Z_1^2 = \sum_{i,k=1}^{N} a_i b_i a_k^* b_k^* \exp j(\theta_i - \theta_k) \tag{A2}$$

similarly

$$Z_2^2 = \sum_{i,k=1}^{N} a_i c_i a_k^* c_k^* \exp j(\theta_i - \theta_k) \tag{A3}$$

$$Z_1^* Z_2 = \sum_{i,k=1}^{N} a_i b_i a_k^* c_k^* \exp j(\theta_k - \theta_i)$$

Substituting A2, A3, and A4 into 4 yields,

$$\gamma^2(\omega) = \frac{\left| \left[\sum_{i,k=1}^{N} a_i b_i a_k^* c_k^* \int_{-\pi}^{\pi} \int_{-\pi}^{\pi} \exp j(\theta_k - \theta_i + K_k \cos\theta_k + K_i \cos\theta_i) d\theta_i d\theta_k \right] \right|^2}{\left[\sum_{i,k=1}^{N} a_i b_i a_k^* b_k^* \int_{-\pi}^{\pi} \int_{-\pi}^{\pi} \exp j(\theta_i - \theta_k + K_k \cos\theta_k + K_i \cos\theta_i) d\theta_i d\theta_k \right] \cdot} \tag{A4}$$

$$\left[\sum_{i,k=1}^{N} a_i c_i a_k^* c_k^* \int_{-\pi}^{\pi} \int_{-\pi}^{\pi} \exp j(\theta_i - \theta_k + K_k \cos\theta_k + K_i \cos\theta_i) d\theta_i d\theta_k \right]$$

To evaluate A4 we need to evaluate integrals in the form

$$I = \int_{-\pi}^{\pi} [\exp j(\theta + K\cos\theta)/2\pi] d\theta$$

$$= \frac{1}{\pi}\int_{o}^{\pi} \cos\theta \exp(K\cos\theta) d\theta \qquad \text{(A5)}$$

$$= I_1(K)$$

See page 376 of Abramowitz and Stegun[8] for the evaluation of the integral. Substituting this result in Equation A4 and setting N=2 produces Equation 5. This substitution requires that the θ_i are independent.

APPENDIX B

COHERENCE SQUARED FOR AMPLITUDE FLUCTUATIONS

For amplitude fluctuations the signal coherence is evaluated in a manner analegous to that for phase fluctuations. It is necessary to evaluate,

$$\left| \overline{Z_1^2(\omega)} \right| = \int_0^{2\alpha} Z_1(\omega) Z_2^*(\omega) P(a_1^2) da_1^2 \qquad \text{(B1)}$$

To simplify the evaluation we specialize to two modes. We also use the fact that the distribution of a_2 is specified by the distribution of a_1^2 i.e. $a_2^2 = 1-a_1^2$, first evaluating coherence for source motion perpendicular to the line joining source and receivers.

Expanding B1 we have,

$$\left| \overline{Z_1^2(\omega)} \right| = \int_0^{2\alpha} (a_1^2 b_1^2 + 2a_1 a_2 b_1 b_2^* + a_2^2 b_2^2) P(a_1^2) da_1^2$$

Let $x = a_1^2$ then,

$$= b_1^2 \int_0^{2\alpha} xP(x)dx + 2b_1 b_2 \int_0^{2\alpha} \sqrt{x(1-x)}\, P(x)dx + b_2^2 \int_0^{2\alpha} (1-x)P(x)dx \qquad \text{(B2)}$$

similarly

$$\overline{Z_1(\omega)Z_2^*(\omega)} = \int_0^{2\alpha} (a_1^2 b_1 c_1^* + a_1 a_2 (b_2 c_1^* + b_1 c_2^*) + a_2^2 b_2 c_2^*) P(a_1^2) da_1^2$$

$$= b_1 c_1^* \int_0^{2\alpha} xP(x)dx + (b_2 c_1^* + b_1 c_2^*) \int_0^{2\alpha} \sqrt{x(1-x)}\, P(x)dx$$

$$+ b_2 c_2^* \int_0^{2\alpha} (1-x)P(x)dx \qquad \text{(B3)}$$

Thus it is necessary to evaluate

(a) $\int_0^{2\alpha} xP(x)dx$

(b) $\int_0^{2\alpha} (1-x)P(x)dx$

(c) $\int_0^{2\alpha} \sqrt{x(1-x)}\, P(x)dx$

(a) Clearly $\int_0^{2\alpha} xP(x)dx = \alpha$

(b) From (a) it follows that $\int_0^{2\alpha} (1-x)P(x)dx = 1-\alpha$

(c) $$\int_0^{2\alpha} \sqrt{x(1-x)}\, P(x)dx = \frac{1}{2\alpha I_o(K)} \int_0^{2\alpha} \sqrt{x(1-x)}\, \exp(-K\cos(\pi x/\alpha))dx \qquad \text{(B4)}$$

$$= \beta$$

To evaluate this integral numerical evaluation was used except in the case where $\alpha = 0.5$. For $\alpha = 0.5$,

$$\beta = \frac{1}{I_o(K)} \int_0^{1} \sqrt{x(1-x)}\, \exp(-K\cos(2\pi x))dx$$

We can write $\sqrt{x(1-x)}$ as a Fourier series by using expressions given in Gradshteyn[9] pp. 425, 1059,

$$\beta = \frac{\pi}{8I_o(K)} \int_o^1 \exp(-K\cos 2\pi x)dx + \frac{1}{2I_o(k)} \sum_{n=1}^{\infty} J_1\frac{(\pi n)(-1)^n}{n} \int_o^1 \exp(-K\cos(2\pi x))\cos 2\pi nx dx \tag{B5}$$

Let $y = 2\pi x$

$$= \frac{1}{8I_o(K)} \int_o^{\pi} \exp(-K\cos y)dy + \frac{1}{2\pi I_o(K)} \sum_{n=1}^{\infty} \frac{J_1(\pi n)(-1)^n}{n} \cdot \int_o^{\pi} \exp(-K\cos y)\cos nydy.$$

$$\beta = \pi/8 + \frac{1}{2I_o(K)} \sum_{n=1}^{\infty} \frac{J_1(\pi n)I_n(K)}{n} \tag{B6}$$

The results from Equations B5, B6 and B9 are substituted into B1 and B2. The result is then substituted into 4 to give Equation 7.